Science of the Total Environment 947 (2024) 174345

Contents lists available at ScienceDirect

Science of the Total Environment

journal homepage: www.elsevier.com/locate/scitotenv

Marine heatwaves alter competition between the cultured macroalga *Gracilariopsis lemaneiformis* and the harmful bloom alga *Skeletonema costatum*

Lin Gao [a], Yonglong Xiong [a], Fei-Xue Fu [b], David A. Hutchins [b], Kunshan Gao [a], Guang Gao [a,*]

[a] State Key Laboratory of Marine Environmental Science & College of Ocean and Earth Sciences, Xiamen University, Xiamen 361005, China
[b] Marine and Environmental Biology, University of Southern California, Los Angeles, CA, United States

HIGHLIGHTS

- Growth and photosynthesis of *G. lemaneiformis* was greatly reduced by heatwave.
- *G. lemaneiformis* did not recover even after one week recovery.
- Growth of *S. costatum* was also reduced but returned to normal after the heatwave.
- The decline in *S. costatum* was related to allelochemical release from the seaweed.
- *S. costatum* responded to the stressful environment by forming aggregates.

GRAPHICAL ABSTRACT

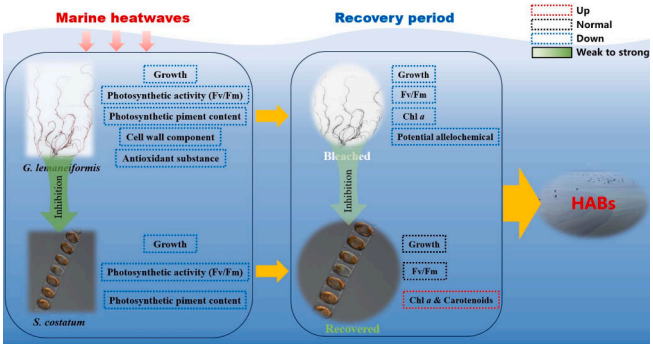

ARTICLE INFO

Editor: Kyle Bibby

Keywords:
Algal bloom
Allelopathy
Marine heatwaves
Metabolomics
Physiological response
Seaweed culture

ABSTRACT

Seaweed cultivation can inhibit the occurrence of red tides. However, how seaweed aquaculture interactions with harmful algal blooms will be affected by the increasing occurrence and intensity of marine heatwaves (MHWs) is unknown. In this study, we run both monoculture and coculture systems to investigate the effects of a simulated heatwave on the competition of the economically important macroalga *Gracilariopsis lemaneiformis* against the harmful bloom diatom *Skeletonema costatum*. Coculture with *G. lemaneiformis* led to a growth decrease in *S. costatum*. Growth and photosynthetic activity (F_v/F_m) of *G. lemaneiformis* was greatly reduced by the heatwave treatment, and did not recover even after one week. Growth and photosynthetic activity of *S. costatum* was also reduced by the heatwave in coculture, but returned to normal during the recovery period. *S. costatum* also responded to the stressful environment by forming aggregates. Metabolomic analysis suggests that the negative effects on *S. costatum* were related to an allelochemical release from *G. lemaneiformis*. These findings show that MHWs may enhance the competitive advantages of *S. costatum* against *G. lemaneiformis*, leading to more severe harmful algal blooms in future extreme weather scenarios.

* Corresponding author.
E-mail address: guang.gao@xmu.edu.cn (G. Gao).

https://doi.org/10.1016/j.scitotenv.2024.174345
Received 9 April 2024; Received in revised form 12 June 2024; Accepted 26 June 2024
Available online 1 July 2024

1. Introduction

Marine heatwaves (MHWs) are extreme warm water events that have been defined as the daily sea surface temperature (SST) exceeding the 90 % threshold relative to a 30-year historical baseline period, and lasting at least 5 days (Hobday et al., 2016). The intensification of global warming makes the occurrence of MHWs more frequent and intense with longer duration (Viglione, 2021). From 1925 to 2016, the frequency and duration of global average MHWs increased by 34 % and 17 % respectively, and the number of days of global average annual MHWs increased by 54 % (from 26 days to 40 days) (Oliver et al., 2018). China is suffering from severe MHWs. The frequency of MHWs in China's marginal seas is nearly twice higher than the global average (Yao et al., 2020).

The impacts of MHWs on the marine ecosystem are receiving increased attention. MHWs are an important driver that leads to coral bleaching (Donovan et al., 2021), and can also have a profound impact on marine biological community structure (Wernberg et al., 2013), biodiversity (Wernberg et al., 2016), marine carbon fixation and storage capacity (Barton et al., 2020; Gao et al., 2021; Jiang et al., 2024), ecosystem services and aquaculture (Barbeaux et al., 2020; Evans et al., 2020; Pershing et al., 2018). Some of these effects of MHWs can have irreparable consequences for the marine environment (Smale and Wernberg, 2013; Wernberg, 2021).

Harmful algal blooms (HABs) or “red tides” represent environmentally or economically damaging microalgal blooms that can occur when conditions are favorable. The worldwide occurrence of HABs shows a rising trend, due mainly to eutrophication and climate change (Dai et al., 2023; Fu et al., 2012). The decay of a dense HAB can often deplete the oxygen in seawater, forming hypoxic or anoxic ‘dead zones’ that can cause the death of fish and invertebrates, resulting in ecosystem degradation (Heil and Muni-Morgan, 2021). In addition, the toxins produced by some HAB species can accumulate in the food web, causing illness or mortality of marine species (Hoagland et al., 2020) and leading to the closure of fisheries and aquaculture as well as negative effects on the tourism industry (Bechard, 2020).

Seaweed cultivation has a long history in Asia, and the scale of macroalgal aquaculture continues to rise to meet increased demand from the food and feed industries (Hwang et al., 2019). In addition, trials of seaweed culture are also being conducted in America and Europe to test its possible role in biofuel production and carbon sequestration (Duarte et al., 2022). In addition to the applications mentioned above, seaweed cultivation has been proven to decrease the occurrence of HABs via nutrient competition (Chai et al., 2018; Gao et al., 2019a). Previous studies have shown that macroalgae can also inhibit growth of harmful species by secreting allelochemicals (Accoroni et al., 2015; Jeong et al., 2000; Nan et al., 2004). Therefore, seaweed cultivation may be a natural solution to deal with HABs. However, it was reported that red tides could occur in seaweed cultivation areas in recent years (Li et al., 2023). Whether this change was caused by MHWs and how MHWs would affect the inhibitory activity of seaweed cultivation on harmful blooms remain unknow.

Based on previous studies, we hypothesize that MHWs may weaken the inhibition of HAB species by cultivated seaweeds, given their differential responses to thermal stress. *G. lemaneiformis* is an important cultivated seaweed in China, having a production of 610,824 t DW in 2022 (CFSY, 2023). *S. costatum* is a widespread HAB species and accounts for the highest occurrences of diatom HABs in China (Feng et al., 2024). Although it does not make toxins, *S. costatum*'s blooms can cause severe environmental harm and economic losses (Shen et al., 2012). Previous study shows that *G. lemaneiformis* can significantly inhibit the occurrence of *S. costatum* HABs (Yang et al., 2015). In this study, *G. lemaneiformis* and *S. costatum* were grown in a simulated MHW in different culture systems to test the hypothesis mentioned above. Both physiological and molecular responses were analyzed to contribute to our limited current understanding of the interactions between cultivated seaweeds and HABs under MHWs.

2. Materials and methods

2.1. Algal collection and algae culture

G. lemaneiformis was collected from a seaweed farm at Ningde (119.31°E, 26.39°N), Fujian province of China in November 2022. After being transported back to the laboratory, *G. lemaneiformis* was thoroughly washed with 0.22 μm filtered natural seawater to remove surface attachments. The macroalgae were precultured in a laboratory incubator (HP200G-3 light incubator, Ruihua, Wuhan, China) for two weeks at 20 °C and a light intensity of 100 μmol photons m^{-2} s^{-1} (L:D = 12:12). The 40 % f/2 medium (Guillard and Ryther, 1962) was renewed half every three days for a semicontinuous culture to supply enough nutrients (Fig. S1). For experiments, *G. lemaneiformis* with similar side branches were selected, and the thalli were gently wiped with degreased cotton dipped in sterilized natural seawater to remove other algae that might attach to the surface of the thallus.

Skeletonema costatum (Cleve 1900) was obtained from the Center for Collections of Marine Algae (CCMA) at the State Key Laboratory of Marine Environmental Science of Xiamen University. Before the experiment, it was also treated with double antibiotics (200 U mL^{-1} penicillin and 0.2 mg mL^{-1} streptomycin) for 24 h, to remove bacteria as much as possible because bacterial proliferation can affect growth of *S. costatum*. The culture temperature, light, and other conditions were consistent with *G. lemaneiformis*, and the medium was renewed every 2–3 days according to the cell concentration before the experiment to keep cells in the exponential growth phase.

2.2. Experimental design

Both coculture and monoculture systems were set up in this study. Coculture system included *G. lemaneiformis* and *S. costatum*, while the monoculture system only contained *S. costatum* as a control treatment. Thus, the effects of *G. lemaneiformis* on *S. costatum* were tested by comparing both culture systems. Monoculture of *G. lemaneiformis* was not set because this study aimed to investigate the inhibition of *G. lemaneiformis* on *S. costatum* rather than *S. costatum* on *G. lemaneiformis* under MHWs to test our hypothesis proposed above. Previous studies also show that microalgae, including *S. costatum* and harmful dinoflagellates, cannot inhibit adult seaweeds (Gao et al., 2019a; Liu, 2015). In addition, physiological, morphological, and metabolic performances of both *G. lemaneiformis* and *S. costatum* need to be measured at different time points during 24 days of culture. An additional monoculture will greatly increase the difficulty of measuring the same parameter of different samples in a short time, and decrease the quality of data. The culture container used in the experiment was a 1 L transparent glass conical bottle. The initial density of *G. lemaneiformis* was set to 1 g L^{-1}, similar to the culture density of *G. lemaneiformis* in the aquaculture facility, and the initial cell density of *S. costatum* was set to 1×10^4 cell mL^{-1}, similar to cell densities when *S. costatum* causes a harmful algal bloom (Gao et al., 2019a).

The experiment used a baseline temperature group (20 °C Baseline, 20 °C BL) and a heatwave treatment group (25 °C Heatwave, 25 °C HW). The baseline temperature represents the mean temperature in the seaweed farm of Ningde in April and May when HABs usually occur (Li, 2021). The simulated marine heatwave temperature was set based on local temperature monitoring from 1982 to 2018 and maximum sea surface temperature anomaly could achieve 5 °C (Li et al., 2019; Yao et al., 2020). The baseline temperature was kept at 20 °C throughout the culture period. In heatwave treatment group, temperature was first increased from 20 °C to 25 °C at a rate of 1 °C per day (heatwave heating period), then maintained at 25 °C for one week (heatwave maintenance period), and decreased to 20 °C at a rate of 1 °C per day (heatwave cooling period). The cultures were then maintained at 20 °C for one

week (recovery period), for a total experimental period of 24 days (Fig. S2). Three replicates were included in the baseline group and the heatwave group.

2.3. Measurement of relative growth rate

The fresh weight of *G. lemaneiformis* was measured using an analytical balance (HZK-FA110, HZ, USA) in an ultra-clean workbench. Before weighing, the water on the surface of the thallus was blotted by absorbent paper until the color of the tissue paper did not change and the fresh weight (g) of *G. lemaneiformis* was recorded every three days. The cell density of *S. costatum* was measured using a spectrophotometer at 680 nm. The medium without algal cells was used as the blank reference solution (Doan et al., 2011). A calibration curve was constructed ($R^2 > 0.999$) to calculate cell concentrations (Fig. S3).

The relative growth rates (RGR) of *G. lemaneiformis* and *S. costatum* were calculated according to the formula:

$$\mathrm{RGR}\ (\%\mathrm{d}^{-1}) = (\ln W_t - \ln W_0)/t \times 100\%,$$

where W_t and W_0 are fresh weight for *G. lemaneiformis* or cell density for *S. costatum* on day t and day 0 respectively.

2.4. Measurements of chlorophyll fluorescence parameters

The maximum photochemical efficiency (F_v/F_m) of photosystem II (PSII) was measured by multi-color pulse-amplitude-modulation (Walz, Germany) to evaluate the photosynthetic activity of the algae. For *G. lemaneiformis*, the whole thallus was placed in a sterilized 10 mL centrifuge tube, and seawater from the corresponding culture bottle (filtered by a 0.45 μm cellulose acetate membrane) was added. The thallus was then put in an incubator for dark acclimation for 15 min before determination of F_v/F_m. For *S. costatum*, the algae cells from each treatment condition were placed in a 5 mL centrifuge tube, and were also placed in the original incubator for 15 min dark acclimation before F_v/F_m measurement. The saturation pulse intensity set by the instrument was 8000 μmol photons m^{-2} s^{-1} (800 ms), and the measuring wavelength was 440 nm white light. The intensity of actinic light was consistent with that in the experimental incubator.

2.5. Measurements of photosynthetic pigments

For *G. lemaneiformis*, the contents of Chl *a*, carotenoids, phycoerythrin (PE) and phycocyanin (PC) were measured during the culture period. To better represent the whole thallus, both tip (50 % in weight) and base (50 % in weight) parts of the thallus were collected. About 0.02 g (FW) of thalli were placed in a 15 mL centrifuge tube and incubated in the dark at 4 °C for 24 h after adding 5 mL 100 % methanol. Afterwards, the solution was centrifuged at 8000 r/min at 4 °C for 10 min using a high-speed freezing centrifuge (Universal 320R, Hettich, Germany). The supernatant was taken and measured with an ultraviolet spectrophotometer (TU-1810DASPC, China). The contents of Chl *a* and carotenoids were calculated according to the formulas of Porra et al. (1989) and Strickland and Parsons (1972) respectively:

$$\mathrm{Chl}\ a\ (\mu\mathrm{g\ mL}^{-1}) = 16.29 \times (A_{665} - A_{750}) - 8.54 \times (A_{652} - A_{750})$$

$$\mathrm{Carotenoids}\ (\mu\mathrm{g\ mL}^{-1}) = 7.6 \times [(A_{480} - A_{750}) - 1.49 \times (A_{510} - A_{750})]$$

To determine PE and PC contents in *G. lemaneiformis*, about 0.05 g (FW) thalli and 2.5 mL of 0.1 mol L^{-1} phosphate buffer (pH = 6.8) were added to a glass homogenizer, which were repeatedly ground in an ice box to completely extract phycobiliprotein. The extract with a final volume of 10 mL was transferred to a 15 mL centrifuge tube and centrifuged at 10,000*g* at 4 °C for 10 min by a high-speed freezing centrifuge. The supernatant was taken and the absorption value at a fixed wavelength was determined with phosphate buffer as a blank control. The contents of PE and PC were calculated by the formulas (Beer and Eshel, 1985):

$$\mathrm{PE}\ (\mathrm{mg\ mL}^{-1}) = [(A_{564} - A_{592}) - (A_{455} - A_{592}) \times 0.2] \times 0.12,$$

$$\mathrm{PC}\ (\mathrm{mg\ mL}^{-1}) = [(A_{618} - A_{645}) - (A_{592} - A_{645}) \times 0.51] \times 0.15,$$

where A_{750}, A_{665}, A_{652}, A_{645}, A_{618}, A_{592}, A_{564}, A_{510}, A_{480}, and A_{455} are the absorbance wavelength at 750, 665, 652, 645, 618, 592, 564, 510, 480, and 455 nm, respectively. The pigment content units were then converted into mg g^{-1} FW.

For *S. costatum*, Chl *a* and carotenoid contents were determined during the culture period. About 10 mL of the sample was filtered onto 25 mm GF/F filters (Whatman, USA) and then transferred to a 15 mL centrifuge tube. Five mL of 100 % methanol was added, and the solution was stored it in the dark at 4 °C for 24 h. Afterwards, the extract was centrifuged, measured, and calculated as described above. Chl *a* and carotenoid contents were expressed as pg $cell^{-1}$.

2.6. Measurements of cell aggregation

During the experiment it was observed that there was an obvious aggregation phenomenon for *S. costatum* and thus the number of aggregates of *S. costatum* under different treatment conditions were recorded (Fig. S4). About 2 mL samples were collected and then preserved with Lugol's iodine solution (iodine solution: algae solution =1:100). The aggregates number in 100 μL algal solution, was counted under a microscope using a 100-grid plankton counting frame. To specify the aggregates, the agglomerated particle size of *S. costatum* was divided into three ranges: 50–100 μm, 100–200 μm, and >200 μm. Each sample was counted at least three times, and the average value was taken as the result.

2.7. Measurement of non-targeted metabonomics of G. lemaneiformis

About 0.1 g (FW) thalli of *G. lemaneiformis* were collected with a sterilized 2 mL freezing tube near the highest temperature (14th day), at the end of the heatwave (18th day) and one week after the end of the heatwave (24th day, the last day of the experiment), frozen with liquid nitrogen, and immediately transferred to −80 °C for storage.

The metabolites of the collected samples were extracted and detected by LC-MS (Vanquish Horizon system, Thermo Scientific). In this LC-MS analysis, a UHPLC-Q Exactive HF-X system (Thermo Scientific) was used for non-targeted metabonomics analysis. In addition, 20 μL supernatant was taken from each sample and used as a quality control sample. In the process of instrumental analysis, a QC sample was inserted every 5–15 analysis samples to investigate the stability of the whole detection process. After the completion of the measurement, the original data of LC-MS were imported into the metabonomics processing software Progenesis QI (Waters Corporation, Milford, USA) for baseline filtering, peak identification, integration, retention time correction, peak alignment, etc. A data matrix of retention time, mass-to-charge ratio and peak intensity was obtained, and then the software was used to identify the characteristic peaks. The mass spectrometry information was matched with metabolic databases HMDB (http://www.hmdb.ca/), Metlin (https://metlin.scripps.edu/) and Majorbio Database, and the metabolite information was identified.

Principal component analysis (PCA) and orthogonal least partial squares discriminant analysis (OPLS-DA) were performed on all samples. In addition, student's *t*-test and difference fold analysis were performed. The selection of differential metabolites was determined based on the variable importance in the projection (VIP) obtained from OPLS-DA model and the *p*-value of student's *t*-test. The metabolites with VIP > 1, $p < 0.05$ were defined as differential metabolites. The metabolic pathways of differential metabolites were annotated by KEGG database (https://www.kegg.jp/kegg/pathway.html).

2.8. Data processing and statistical analysis

The experimental data were all expressed by the mean ± standard deviation, statistically analyzed by SPPS 25, and plotted by Origin 2019b software. First, repetitive measure analysis of variance (ANOVA) was used to evaluate the influence of culture time on the measured physiological parameters *G. lemaneiformis* and *S. costatum*. Two-way ANOVA was used to examine the effects on *G. lemaneiformis* and heatwave on physiological parameters of *S. costatum*. Two-tailed *t*-tests were performed to evaluate significant differences in on physiological parameters of *G. lemaneiformis* between heatwave and baseline groups. Least-Significant difference (LSD) was used for post hoc analysis, and the significance level was set at 0.05.

3. Results

3.1. Growth and photosynthesis of G. lemaneiformis and S. costatum

The relative growth rates (RGR) of both algae were first measured (Fig. 1). The RGR of *G. lemaneiformis* grown at baseline and heatwave temperatures showed different pattern with the culture time (p = 0.012), with that at baseline temperature declining initially and then having a stable RGR after day 6, while that at heatwave temperature showed a serious decline in RGR until day 21 (Fig. 1a). Therefore, the RGR at heatwave temperature was significantly lower than that at baseline temperature except for days 3, 6 and 12.

As for *S. costatum* (Fig. 1b), the RGR under different conditions also demonstrated differential patterns (p = 0.001). For monoculture and coculture without heatwave, the RGR decreased with culture time till day 12 and then was stable, while it continuously decreased till day 21 and recovered by day 24 for coculture with heatwave treatment. On day 3, the heatwave treatment increased the RGR of *S. costatum* in the monoculture system but did not affect it in coculture system, probably because the negative effect of the coculture system offset the stimulative effect of heatwave. By day 9, the heatwave condition significantly decreased the RGR of *S. costatum* in the coculture system but not in the monoculture system. The similar pattern was detected on days 18 and 21. By day 24, there were no significant differences between heatwave and non-heatwave treatments.

The maximum photochemical efficiency (F_v/F_m) of *G. lemaneiformis* decreased with culture time, with the heatwave treatment leading to a larger decrease (p = 0.049, Fig. 1c). Therefore, the heatwave significantly decreased F_v/F_m of *G. lemaneiformis* on days 12, 18 and 24. In terms of *S. costatum*, its F_v/F_m also varied with culture time, with that under heatwave in coculture having the largest fluctuation ($p < 0.001$, Fig. 1d). On day 6, coculture reduced F_v/F_m by 6 % at baseline temperature and 11 % under heatwave treatment. On day 18, coculture and heatwave had an interactive effect; heatwave did not affect F_v/F_m in monoculture but reduced it in coculture. Coculture led to the decrease of F_v/F_m on day 24.

3.2. Photosynthetic pigment content of G. lemaneiformis and S. costatum

RM-ANOVA analysis showed that Chl *a* content of *G. lemaneiformis* did not change significantly in the baseline treatment with culture time (p = 0.151, Fig. 2a). However, the heatwave reduced Chl *a* content on days 18 (p = 0.010) and 24 (p = 0.041). A similar trend was found for carotenoids, although heatwave reduced their content only on day 18 (Fig. 2b). PE ($p < 0.001$) and PC (p = 0.001) contents both decreased with culture time in both temperature treatments (Fig. 2c & d). The heatwave treatment reduced PE content on day 18 (p = 0.041) and PC content on days 6 (p = 0.035) and 18 (p = 0.017).

The Chl *a* content of *S. costatum* did not change significantly by day 18, but under coculture+heatwave it was enhanced greatly on day 24 (p = 0.001, Fig. 2e). Coculture increased Chl *a* content on day 6, although it was not statistically significant at the baseline temperature. Coculture also increased Chl *a* content on day 12 for both baseline and heatwave temperatures. Coculture and heatwave had an interactive effect on Chl *a*

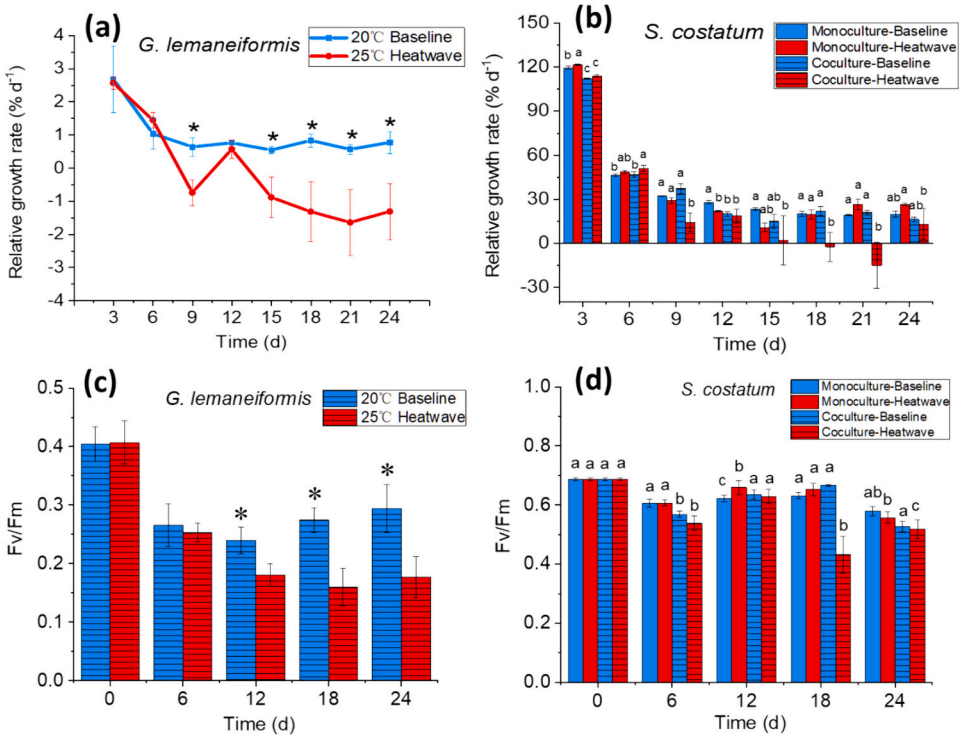

Fig. 1. The relative growth rate (a & b) and F_v/F_m (c & d) of *G. lemaneiformis* and *S. costatum* under heatwave. The value is mean ± standard deviation (SD), * indicates that there is a significant difference between the baseline group and the heatwave group ($p < 0.05$), and different letters indicate that there is a significant difference among different treatment groups ($p < 0.05$).

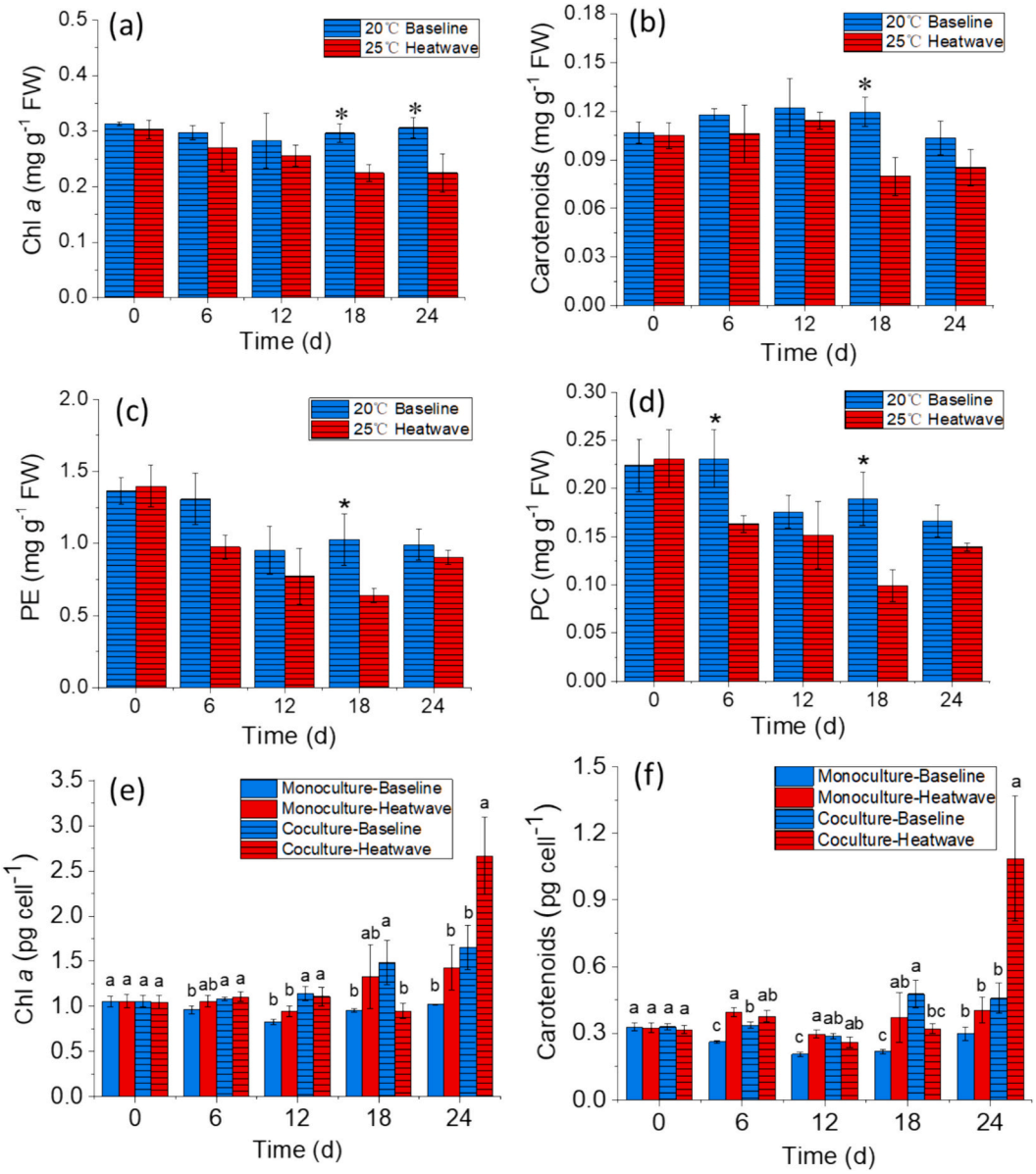

Fig. 2. The photosynthetic piment content of *G. lemaneiformis* (a-d) and *S. costatum* (e & f) in baseline group and heatwave groups. The value is the mean ± standard deviation (SD), * indicates that there is a significant difference between the baseline group and the heatwave group ($p < 0.05$), and different letters indicate that there is a significant difference among different treatment groups ($p < 0.05$).

content on day 18. Heatwave did not affect Chl *a* content in monoculture and reduced it in coculture. Both coculture and heatwave increased Chl *a* content on day 24. Carotenoids content also fluctuated with culture time, with the largest increase occurring under coculture+heawave treatment ($p < 0.001$, Fig. 2f). The heatwave increased carotenoids content in monoculture, but did not have a significant effect in coculture on day 6. A similar trend was detected on day 12. On day 18, the heatwave did not affect carotenoids content in monoculture but reduced it in coculture. On day 24, an opposite effect was found; heatwave did not change carotenoids content in monoculture, but enhanced it dramatically in coculture.

3.3. The agglomeration of S. costatum

Aggregation numbers of *S. costatum* under different treatments increased with culture time until day 12 and then showed a decreasing trend ($p < 0.001$). For 50–100 μm aggregates (Fig. 3a), the heatwave increased aggregation number in coculture but did not affect it in monoculture on day 6. On day 12, there was no significant difference among treatments. On day 18, heatwave decreased aggregation number in coculture but did not affect it in monoculture. On day 24, neither coculture nor heatwave affected algal aggregation. The numbers of aggregates 100–200 μm also varied with culture time but reached the peak at different times for different conditions ($p = 0.004$, Fig. 3b). Both coculture and heatwave stimulated algal aggregation on day 6, while heatwave increased aggregation in monoculture but not in coculture on day 12. In contrast, heatwave reduced algal aggregation in coculture on day 18 and in monoculture on day 24. For aggregates >200 μm (Fig. 3c), aggregation numbers in monoculture increased with culture time but they increased first and then decreased for coculture ($p = 0.009$). Heatwave also enhanced aggregation for both culture systems on day 6. There were no significant differences among treatments on day 12. Heatwave reduced aggregation in coculture, but not in monoculture on day 18. By day 24, coculture and heatwave seemed to reduce algal aggregation but they were not statistically significant.

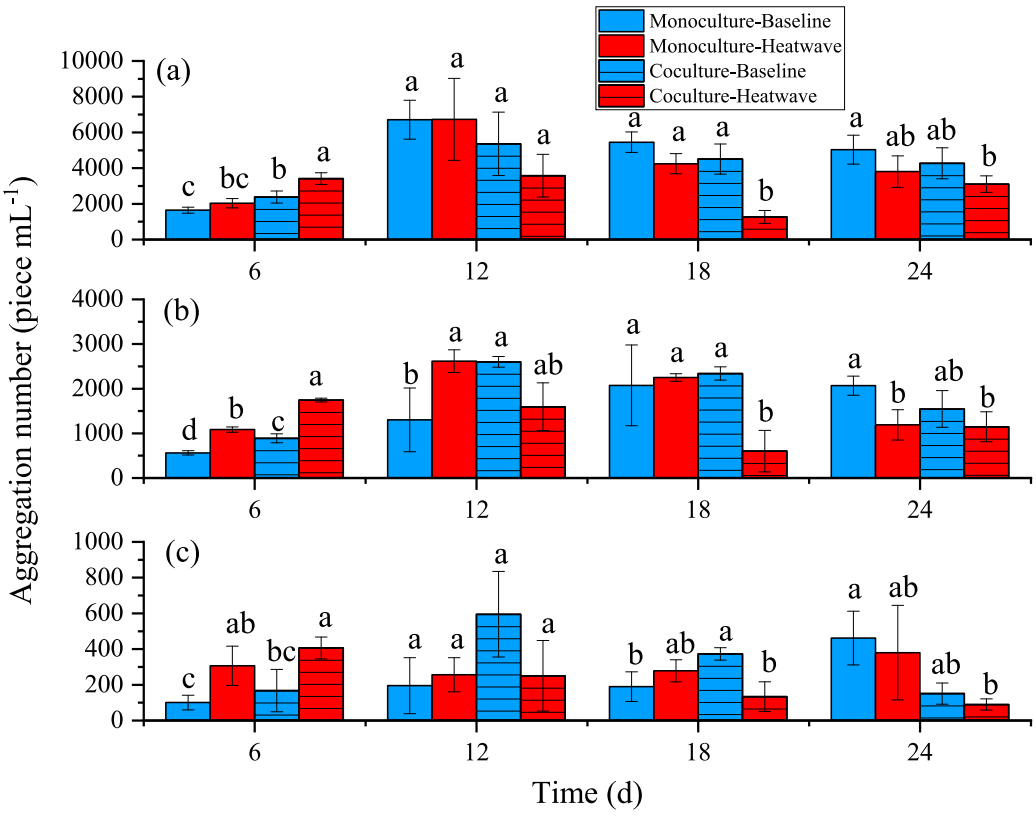

Fig. 3. Aggregation number of *S. costatum* during culture period. (a) Aggregates 50–100 μm, (b) aggregates100–200 μm, and (c) aggregates >200 μm. The value is the mean ± standard deviation (SD), and different letters indicate that there are significant differences among different treatment groups ($p < 0.05$).

3.4. Classification of differential metabolites

Differential metabolites were analyzed in *G. lemaneiformis* between heatwave and baseline temperatures. On day 14, there were 95 differential metabolites detected, with 26 significantly up-regulated and 69 significantly down-regulated (Fig. 4a). The first three types of differential metabolites were organic acids and derivatives, lipids and lipid-like molecules, and organoheterocyclic compounds, which accounted for 27 %, 26 % and 21 % of total metabolites (Fig. 4b). On the 18th day, comparing the heatwave group with the baseline group, there were 122 differential metabolites detected with 36 significantly up-regulated and 86 significantly down-regulated in the heatwave (Fig. 4c). The first three types of differential metabolites were lipids and lipid-like molecules, organoheterocyclic compounds, organic acids and derivatives , which accounted for 29 %, 24 % and 23 % of total metabolites respectively (Fig. 4d). On the 24th day, there were 118 differential metabolites between heatwave and baseline groups, with 85 significantly up-regulated and 33 significantly down-regulated (Fig. 4e). The first three types of differential metabolites were lipids and lipid-like molecules, organoheterocyclic compounds, organic acids and derivatives, which accounted for 51 %, 16 % and 10 % of total metabolites respectively (Fig. 4f).

3.5. Analysis of KEGG pathway of differential metabolites

To clearly understand the effects of MHWs on the metabolic pathways of *G. lemaneiformis*, KEGG enrichment and pathway analysis of different metabolites in *G. lemaneiformis* were carried out at the three sampling points. It turned out that the heatwave significantly affected ABC transporters ($p = 0.016$) and tryptophan metabolism ($p = 0.023$) on the 14th day (Fig. 5a). Indole-3-acetaldehyde and 6-hydroxymelatonin in the tryptophan metabolic pathway were significantly up-regulated by the heatwave, while 5-hydroxyindoleacetate was significantly down-regulated (Fig. 5b). N-succinyl-L,L-2,6-diaminopimelate in the lysine biosynthesis pathway and dihydrophaseic acid in the carotenoid synthesis pathway showed a down-regulation trend (Fig. 5c & d).

On the 18th day, the heatwave significantly affected ABC transporters ($p = 0.010$) and tryptophan metabolism ($p = 0.002$) (Fig. 6a). Indole-3-acetaldehyde, 3-methoxyanthranilate and 6-hydroxymelatonin in the tryptophan metabolic pathway were significantly up-regulated, while 5-hydroxyindoleacetate and 3-hydroxy-L-kynurenine were significantly down-regulated (Fig. 6b). N-succinyl-L,L-2,6-diaminopimelate in lysine biosynthesis pathway and dihydrophaseic acid in the carotenoid synthesis pathway showed a down-regulation trend in the heatwave (Fig. 6 c & d). In addition, D-maltose in the starch and sucrose metabolism pathway and galactosylglycerol in the galactose metabolism pathway were also down-regulated (Fig. 6e & f).

On the 24th day, compared with the baseline group, the metabolic pathway of arachidonic acid in the heatwave group was extremely different ($p < 0.001$) (Fig. 7a), with seven different metabolites (TXB_2, 20-COOH-LTB_4, LXB_4, 14,15-DHET, 11,12-DHET, 11(*R*)-HETE, Hepoxilin A_3) being significantly up-regulated (Fig. 7b). 3-Oxo-2-(2-enenyl) cyclopentaneoctanoic acid (OPC8) in α-linolenic acid metabolism and 9(*S*)-HPODE, 9,12,13-TriHOME in linoleic acid metabolism also showed up-regulation (Fig. 7c & b).

4. Discussion

4.1. Physiological responses of G. lemaneiformis to MHWs in coculture

The experimental results showed that the occurrence of MHWs in the coculture system caused great damage to *G. lemaneiformis*. The thalli showed negative relative growth rates under thermal stress. This damage to algal growth did not disappear even during the recovery period. This destructive influence on growth could be attributed to decreased photosynthetic pigment content and activity of PSII. Thalli also became bleached due to the loss of photosynthetic pigments (Fig. S5), similar to

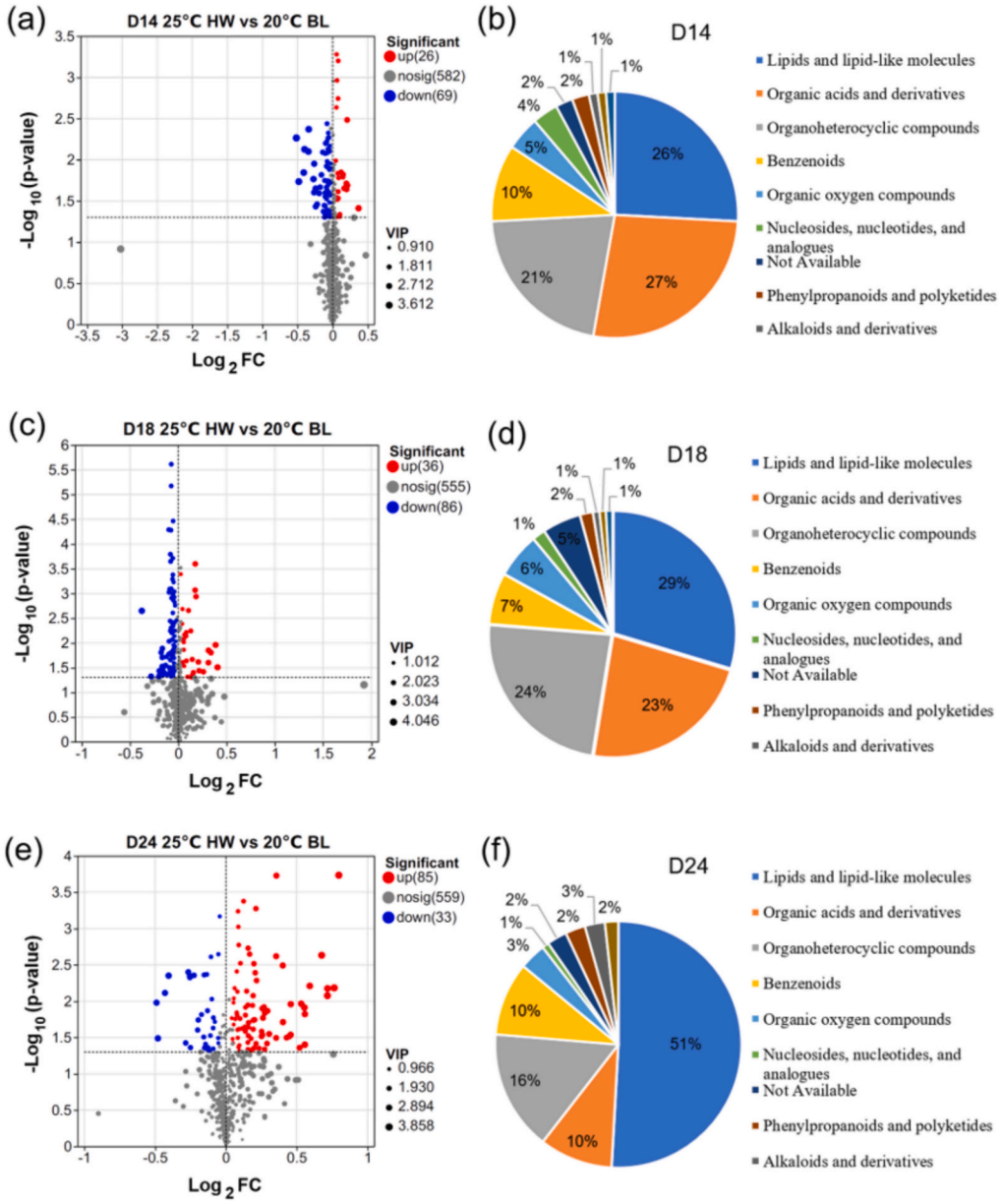

Fig. 4. The scatter plot of different metabolites of *G. lemaneiformis* between the baseline group and the heatwave group on the 14th day (near the highest temperature of the heatwave, a), 18th day (at the end of the heatwave, c) and 24th day (after heatwave recovery, e). Red indicates a significant up-regulation and blue indicates a significant down-regulation. Also shown are the compound classification diagrams of the differential metabolites in *G. lemaneiformis* in the baseline heatwave groups on the 14th (b), 18th (d) and 24th (f) days.

our previous study (Jiang et al., 2022). MHW damage to the photosynthetic activity of macroalgae has been commonly reported, which could be caused by increased ROS under thermal stress (Gao et al., 2021; Nepper-Davidsen et al., 2019). Phycobiliproteins have antioxidative activity and can be induced to scavenge ROS under stressful environments (Cao et al., 2016; Gao et al., 2019b). The contents of PE and PC in this study were reduced under the heatwave condition, which may contribute to increased harm to the photosynthetic activity of *G. lemaneiformis*. The effects of MHWs on relative growth rate of *G. lemaneiformis* can be divided into two stages. In the first stage (days 1–9), the relative growth rate decreased rapidly while the decline trend slowed down with fluctuations in the second stage (days 10–24). These two stages indicate the acclimation of *G. lemaneiformis* to MHWs. The significant recovery of carotenoids, PE and PC contents during the recovery period also supports this acclimation. Whether a longer recovery period can result in a complete recovery of *G. lemaneiformis* remains unknown and needs to be investigated in future.

4.2. Molecular responses of *G. lemaneiformis* to MHWs in coculture

The enrichment of KEGG pathway showed that *G. lemaneiformis* in the heatwave group had significant changes in ABC transporter and tryptophan metabolism pathways on the 14th and 18th day. ABC transporters are a family of membrane proteins that mediate a variety of ATP-driven transport processes (Locher, 2016). They participate in a variety of cellular transport processes for molecules such as ions, sugars, amino acids, vitamins, peptides, polysaccharides and hormones (Jones and George, 2004). Among various ABC transporters, L-Histidine (Holecek, 2020), L-Phenylalanine (Mohy El-Din and El-Ahwany, 2016; Yadavalli et al., 2022) and taurine (Aruoma et al., 1988) have direct or indirect antioxidant effects. The above metabolites were significantly down-regulated in the heatwave group (Tables S1–2), indicating that

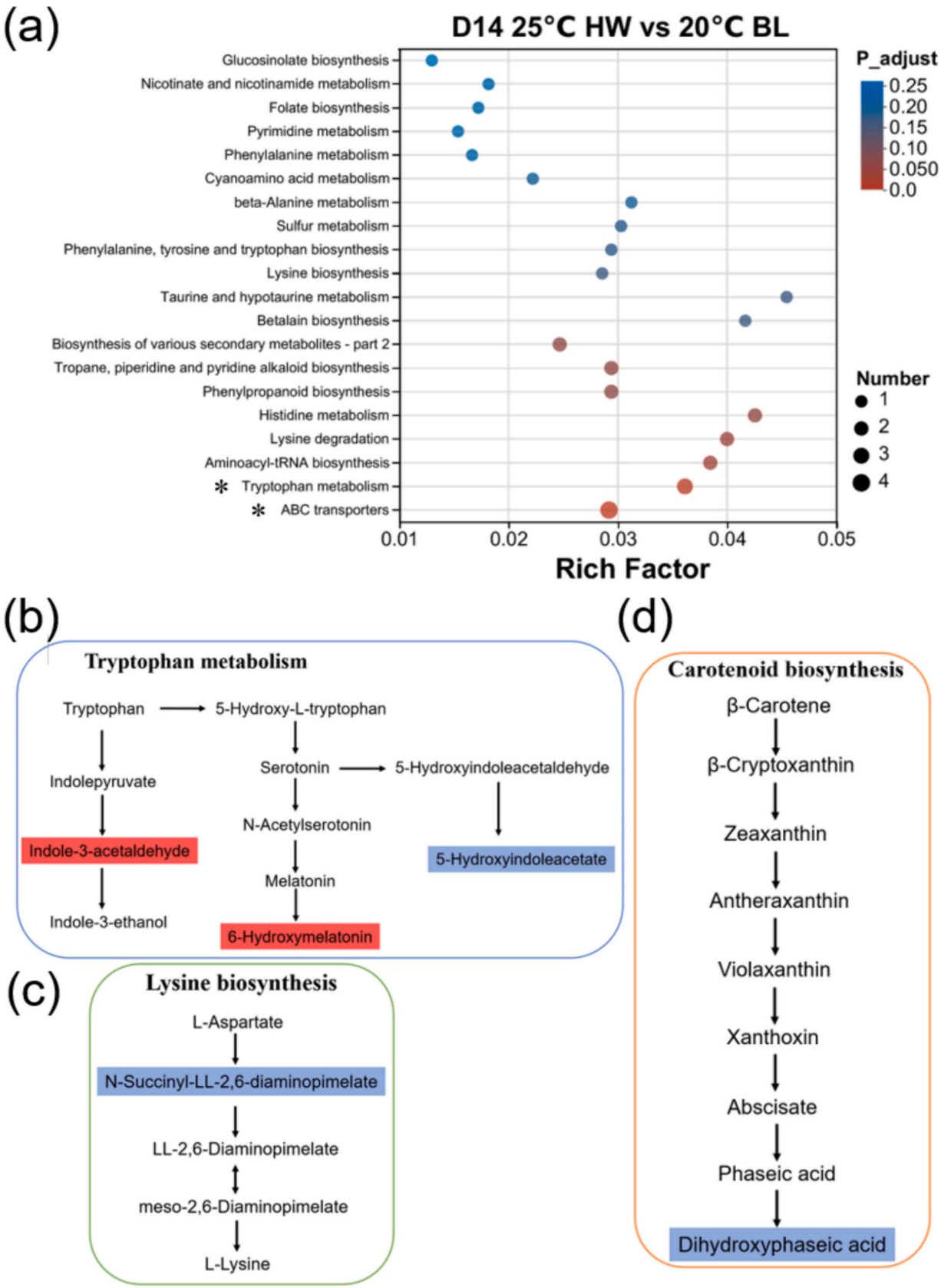

Fig. 5. KEGG analysis of differential metabolites in *G. lemaneiformis* on the 14th day (near the highest temperature of the heatwave). (a) Bubble diagram of KEGG pathway enrichment analysis of differential metabolites. (b) Tryptophan metabolism pathway. (c) Lysine synthesis pathway. (d) Carotenoid synthesis pathway. The * indicates that the differential metabolites in this metabolic pathway are significantly enriched ($p < 0.05$). Red indicates a significant up-regulation and blue indicates a significant down-regulation.

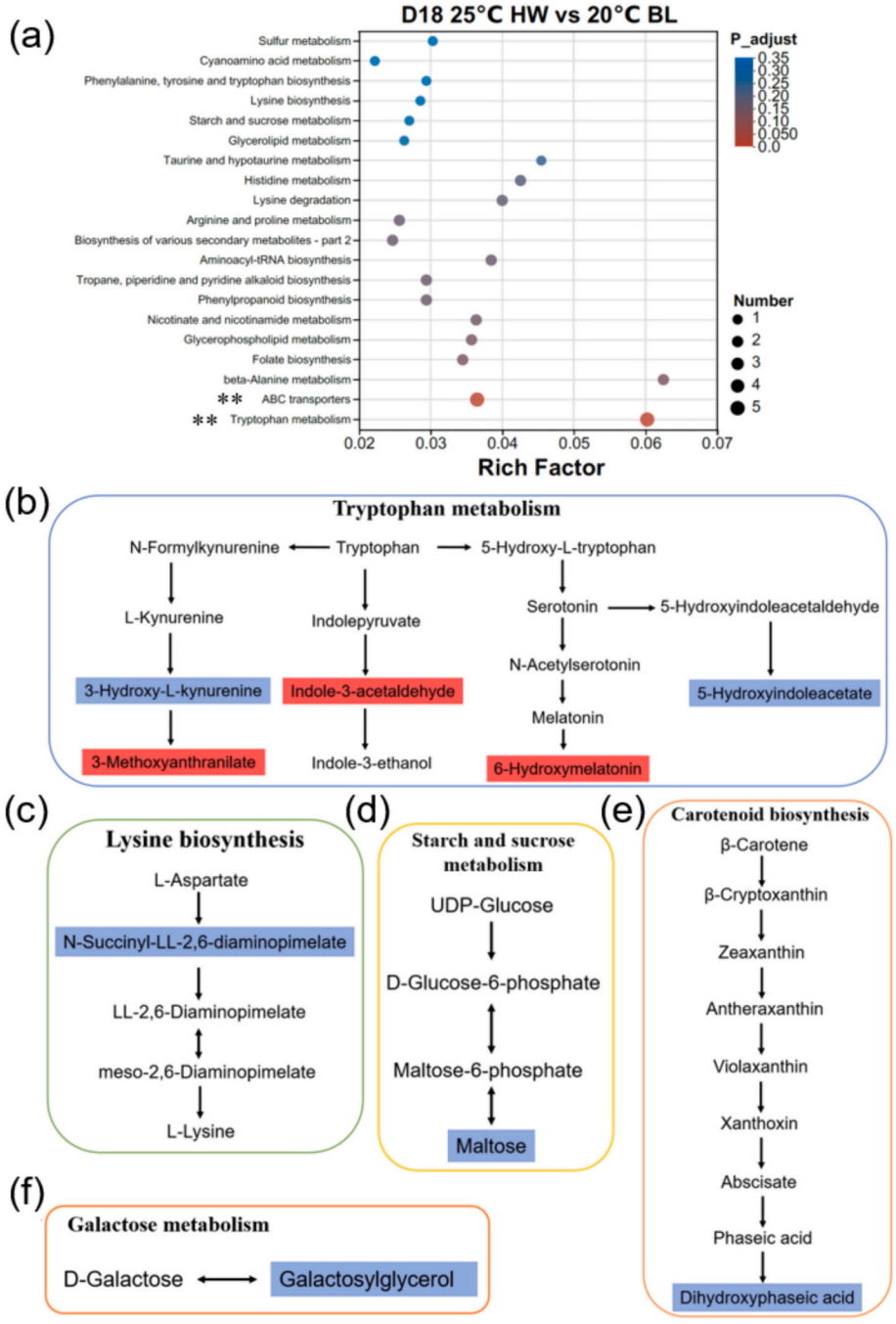

Fig. 6. KEGG analysis of differential metabolites in *G. lemaneiformis* on the 18th day (at the end of heatwave). (a) Bubble diagram of KEGG pathway enrichment analysis of differential metabolites. (b) Tryptophan metabolism pathway. (c) Lysine synthesis pathway. (d) Starch and sucrose metabolism pathway. (e) Carotenoid synthesis pathway. (f) Galactose metabolism pathway. The ** indicates that the differential metabolites in this metabolic pathway are extremely significantly enriched ($p < 0.01$). Red indicates a significant up-regulation and blue indicates a significant down-regulation.

heatwaves might damage the antioxidant capacity of *G. lemaneiformis*. In addition, the down-regulation of dihydrohexaenoic acid in the synthetic pathway of carotenoids that have antioxidant activity was also detected on the 14th and 18th days. The physiological results also showed that the carotenoids content of *G. lemaneiformis* in the heatwave group was lower than that in the baseline group, indicating that the antioxidant capacity of *G. lemaneiformis* decreased at the maximum temperature and at the end of the heatwave. The decreased antioxidant capacity could contribute to the reduced photosynthetic performance and growth of *G. lemaneiformis*.

The adjustment of fatty acid composition is an important response mechanism of algae to environmental change (Sanina et al., 2008; Schmid et al., 2020). The classification analysis in this study also showed that the changes of metabolites in *G. lemaneiformis* were mainly concentrated in lipids and lipid-like molecules. Many previous studies have shown that temperature changes directly affect the fatty acid composition of macroalgae and thus their growth and development (Santos et al., 2017; Tala and Chow, 2014; Uji et al., 2013). When subjected to MHWs stress, algae usually increased the content of saturated fatty acids (SFA) and decreased the content of polyunsaturated fatty acids (PUFA), so as to reduce the membrane fluidity to resist the negative effects of temperature rise (Britton et al., 2020; Svenning et al.,

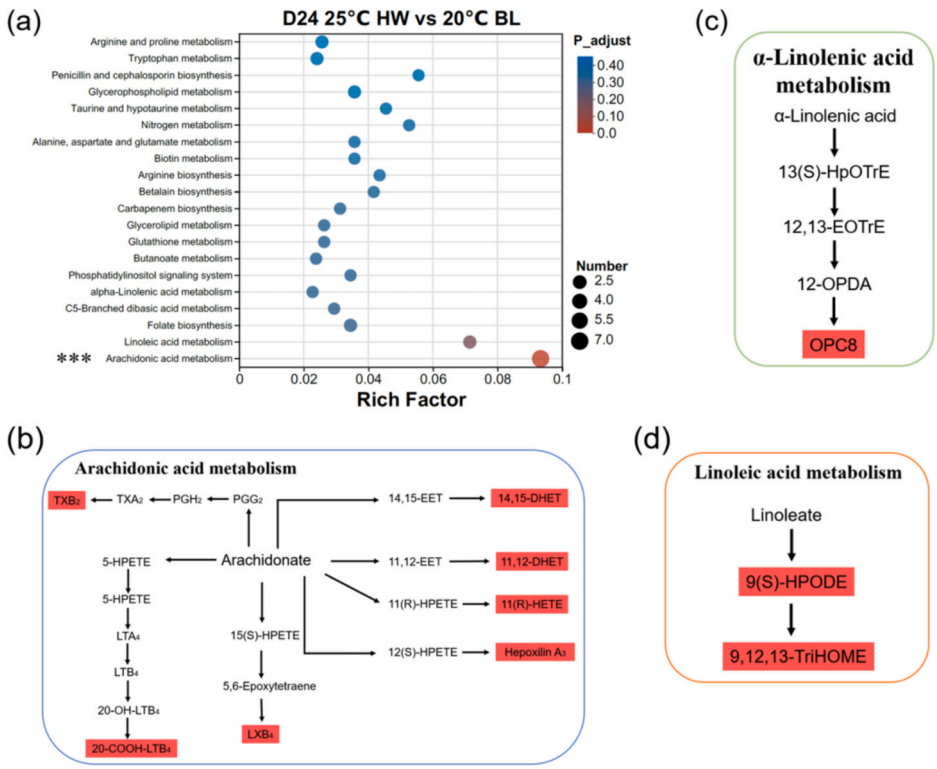

Fig. 7. Analysis of differential metabolites of *G. lemaneiformis* on the 24th day (after heatwave recovery). (a) Bubble diagram of KEGG pathway enrichment analysis of differential metabolites. (b) Arachidonic acid metabolism pathway. (c) α-Linolenic acid metabolism pathway. (d) Linoleic acid metabolism pathway. The *** indicates that the differential metabolites in this metabolic pathway are significantly enriched ($p < 0.001$). Red indicates a significant up-regulation and blue indicates a significant down-regulation.

2019). In this study, the degradation of PUFA including arachidonic acid, α-linolenic acid and linoleic acid was also detected on day 24. The decrease of cell membrane fluidity may lead to the weakening of electron transfer in photosystems and the decrease of photosynthesis of *G. lemaneiformis*, which was supported by the decreased F_v/F_m of *G. lemaneiformis* in the heatwave group.

4.3. Effects of MHWs on S. costatum and its competition with G. lemaneiformis

For *S. costatum*, at most timepoints in the monoculture system the occurrence of MHWs increased its relative growth rate and its pigment content also increased slightly, indicating that the simulated MHW had a positive impact on *S. costatum*. Previous studies also show that high temperature during heatwaves could aggravate phytoplankton blooms and cause serious consequences to the ecosystem (Huang et al., 2021; Kling et al., 2020; Kelly et al., 2023; Lopes et al., 2023; Roberts et al., 2019). On the other hand, MHWs led to a significant decrease in relative growth rate of *S. costatum* in coculture on days 9, 18 and 21. Considering the contrary effects of MHWs on *S. costatum* between monoculture and coculture, this decrease in growth should be related to the presence of *G. lemaneiformis*. Meanwhile, F_v/F_m and photosynthetic pigment content of *S. costatum* were also reduced on day 18 in coculture. It seems that *G. lemaneiformis* inhibited the growth of *S. costatum* by damaging its photosynthetic activity. However, relative growth rate of *G. lemaneiformis* was also reduced by MHWs on days 9, 18 and 21. How did *G. lemaneiformis* impose negative effects on *S. costatum*? Previous studies show that both fresh and dried *G. lemaneiformis* can inhibit photosynthesis and growth of HAB algae by allelopathic effects (Wang et al., 2007; Ye et al., 2014). Therefore, both healthy and unhealthy thalli of *G. lemaneiformis* can impose negative effects on microalgae by releasing allelochemicals actively or passively. D-galactose is a soluble substance involved in cell wall formation of many red algae (Li et al., 2002), and it is also a protective agent for maintaining cell osmotic balance (Hoef-Emden, 2014). Meanwhile, maltose has the ability to protect the cytomembrane at physiologically relevant concentrations (Kaplan and Guy, 2004). In this study, both D-galactose and maltose were down-regulated in the heatwave treatment, suggesting damage to the cell wall and cytomembrane. Therefore, there is high possibility that a lot of intracellular substances in *G. lemaneiformis*, including allelochemicals, were released to the water environment, inhibiting photosynthetic activity and growth of *S. costatum*.

After one-week recovery period, relative growth rate of *S. costatum* cultured under heatwave in coculture recovered to the same level as that without heatwave treatment. This recovery could be due to the decreased inhibition by *G. lemaneiformis*. On the other hand, the relative growth rate of *G. lemaneiformis* did not recover by the end of the experiment, maintaining negative growth rates. This suggests that the heatwave caused severe damage to *G. lemaneiformis.* This damage can potentially affect both the synthesis of some metabolites and accelerate their degradation. As shown in the metabolome analysis, synthesis of arachidonic acid, α-linolenic acid and linoleic acid in *G. lemaneiformis* was up-regulated, suggesting that these three compounds were transformed to other substances. Arachidonic acid is the main polyunsaturated fatty acid in red algae (Al-Hasan et al., 1991; Khotimchenko et al., 1991; Santos et al., 2017). Previous studies have shown that linolenic acid in *Sargassum fusiforme* had significant allelopathic effects on the HAB raphidophyte *Heterosigma akashiwo*. High concentrations of linolenic acid reduced the activities of antioxidant enzymes such as superoxide dismutase (SOD) and peroxidase (POD) in *Heterosigma akashiwo*, and the photosynthetic pigment content, F_v/F_m and $rETR_{max}$ of microalgae also gradually decreased with the increase of linolenic acid concentration (Sun et al., 2021). After the heatwave, the degradation of linolenic acid was intensified and the content of polyunsaturated fatty

acids was reduced, which indicated that the allelochemicals of *G. lemaneiformis* which have inhibitory effects on *S. costatum* were significantly reduced, leading to the recovery of *S. costatum*.

An interesting phenomenon is that coculture and heatwave treatments could affect aggregation of *S. costatum*. Aggregation is a strategy for microalgae to respond to stressful environments (Calla, 2022). For instance, the unicellular green alga *Chlamydomonas reinhardtii* forms aggregates in response to predation and chemical exposure (Herron et al., 2019). In this study, coculture resulted in significant aggregation of *S. costatum* compared to monoculture by day 6. This suggests that coculture with *G. lemaneiformis* induced this aggregation phenomenon. However, this phenomenon disappeared on days 12, 18 and 24 and coculture with the heatwave even led to decreased aggregation, particularly on days 12 and 18. This may be caused by allelochemicals released by *G. lemaneiformis*. Allelochemicals could reduce cell aggregation of *S. costatum* and thus increase the inhibitory effect on it. The heatwave also induced more aggregation on day 6, which could be attributed to its stimulative effect on growth of *S. costatum* or stickier cell surface on higher temperatures since high cell density can also result in cell aggregation (Thornton and Thake, 1998).

4.4. Differential responses of G. lemaneiformis and S. costatum to MHWs

G. lemaneiformis maintained a negative relative growth rate after day 15, and did not recover even after one-week. It seems that the heatwave imposed permanent damage on *G. lemaneiformis*. It has been found that high-intensity MHWs could led to species extinctions when they exceed the thermal thresholds of seaweeds (Hereward et al., 2020; Smale and Wernberg, 2013). On the other hand, the relative growth rate of *S. costatum* turned from negative to positive and recovered to a similar level with that without heatwave by the end of the recovery period, showing a strong resilience. Patil et al. (2020) found that *Pyropia haitanensis* can significantly inhibit the growth of *S. costatum*, but some of *S. costatum* cells still survived at very low density. Compared with macroalgae, microalgae can be deemed as *r*-strategists (Gao et al., 2019a). *r*-strategists generally have small sizes and short life spans but can survive unstable and drastic environments due to a large number of individuals. They can also thrive again via rapid reproduction when the environment is back to normal (Gao et al., 2019a; Papanikolopoulou et al., 2018). Therefore, the differential responses of *G. lemaneiformis* and *S. costatum* to heatwaves can be attributed to their inherent features and survival strategies. Based the findings in the present study, MHWs can weaken the competition of *G. lemaneiformis* against *S. costatum,* and may lead to more severe harmful algal blooms in future climate change scenarios.

5. Conclusion

Seaweed cultivation can impose an inhibitory effect on the occurrence of harmful bloom algae through competition and allelopathy. This study investigates the effects of MHWs on these competitive interactions of cultivated seaweeds and red tide microalgae. The simulated heatwave led to a growth decrease of *G. lemaneiformis* and thallus bleaching. The likely release of allelochemicals from *G. lemaneiformis* caused the significant inhibition of photosynthetic activity and growth in *S. costatum*. After the simulated heatwave disappeared, *S. costatum* was able to recover its growth and thrive, while *G. lemaneiformis* continued to decay. The findings in this study indicate that the reduced inhibition of macroalgae on microalgae caused by MHWs may lead to more severe harmful algal blooms in future extreme weather scenarios.

CRediT authorship contribution statement

Lin Gao: Writing – review & editing, Writing – original draft, Visualization, Methodology, Investigation, Formal analysis, Data curation. **Yonglong Xiong:** Writing – review & editing, Methodology, Investigation, Formal analysis, Data curation. **Fei-Xue Fu:** Writing – review & editing, Validation, Methodology, Formal analysis. **David A. Hutchins:** Writing – review & editing, Validation, Methodology, Formal analysis. **Kunshan Gao:** Writing – review & editing, Validation, Methodology, Formal analysis. **Guang Gao:** Writing – review & editing, Writing – original draft, Visualization, Validation, Supervision, Resources, Methodology, Funding acquisition, Formal analysis, Conceptualization.

Declaration of competing interest

The authors declare that they have no known competing financial interests or personal relationships that could have appeared to influence the work reported in this paper.

Data availability

Data will be made available on request.

Acknowledgments

This work was supported by the National Natural Science Foundation of China (42076154), the National Key Research and Development Program of China (2022YFC3105304), the Natural Science Foundation of Fujian Province (2022J01026, 2021J01026), and the MEL Internal Research Program (MELRI2304). The authors are grateful to the laboratory technicians Wenyan Zhao and Xianglan Zeng for their logistical and technical support.

Appendix A. Supplementary data

Supplementary data to this article can be found online at https://doi.org/10.1016/j.scitotenv.2024.174345.

References

Accoroni, S., Percopo, I., Cerino, F., Romagnoli, T., Pichierri, S., Perrone, C., Totti, C., 2015. Allelopathic interactions between the HAB dinoflagellate *Ostreopsis cf. ovata* and macroalgae. Harmful Algae 49, 147–155.

Al-Hasan, R.H., Hantash, F.M., Radwan, S.S., 1991. Enriching marine macroalgae with eicosatetraenoic (arachidonic) and eicosapentaenoic acids by chilling. Appl. Microbiol. Biotechnol. 35, 530–535.

Aruoma, O.I., Halliwell, B., Hoey, B.M., Butler, J., 1988. The antioxidant action of taurine, hypotaurine and their metabolic precursors. Biochem. J. 256, 251–255.

Barbeaux, S.J., Holsman, K., Zador, S., 2020. Marine heatwave stress test of ecosystem-based fisheries management in the Gulf of Alaska pacific cod fishery. Front. Mar. Sci. 7, 703.

Barton, S., Jenkins, J., Buckling, A., Schaum, C.E., Smirnoff, N., Raven, J.A., Yvon-Durocher, G., 2020. Evolutionary temperature compensation of carbon fixation in marine phytoplankton. Ecol. Lett. 23, 722–733.

Bechard, A., 2020. The economic impacts of harmful algal blooms on tourism: an examination of Southwest Florida using a spline regression approach. Nat. Hazards 104, 593–609.

Beer, S., Eshel, A., 1985. Determining phycoerythrin and phycocyanin concentrations in aqueous crude extracts of red algae. Mar. Freshw. Res. 36 (6), 785–792.

Britton, D., Schmid, M., Noisette, F., Havenhand, J.N., Paine, E.R., McGraw, C.M., Revill, A.T., Virtue, P., Nichols, P.D., Mundy, C.N., Hurd, C.L., 2020. Adjustments in fatty acid composition is a mechanism that can explain resilience to marine heatwaves and future ocean conditions in the habitat-forming seaweed *Phyllospora comosa* (Labillardière) C. Agardh. Glob. Chang. Biol. 26, 3512–3524.

Calla, B., 2022. Stronger together: how unicellular algae respond to stress by socialization. Plant Physiol. 192 (3), 1554–1555.

Cao, J., Wang, J., Wang, S., Xu, X., 2016. *Porphyra* species: a mini-review of its pharmacological and nutritional properties. J. Med. Food 19 (2), 111–119.

CFSY, 2023. China Fishery Statistical Yearbook. China Agriculture Press, Beijing, p. 2023.

Chai, Z.Y., He, Z.L., Deng, Y.Y., Yang, Y.F., Tang, Y.Z., 2018. Cultivation of seaweed *Gracilaria lemaneiformis* enhanced biodiversity in a eukaryotic plankton community as revealed via metagenomic analyses. Mol. Ecol. 27, 1081–1093.

Dai, Y., Yang, S., Zhao, D., Hu, C., Xu, W., Anderson, D.M., Li, Y., Song, X.P., Boyce, D.G., Gibson, L., Zheng, C., 2023. Coastal phytoplankton blooms expand and intensify in the 21st century. Nature 615 (7951), 280–284.

Doan, T.T.Y., Sivaloganathan, B., Obbard, J.P., 2011. Screening of marine microalgae for biodiesel feedstock. Biomass Bioenergy 35 (7), 2534–2544.

Donovan, M.K., Burkepile, D.E., Kratochwill, C., Shlesinger, T., Sully, S., Oliver, T.A., Hodgson, G., Freiwald, J., van Woesik, R., 2021. Local conditions magnify coral loss after marine heatwaves. Science 372 (6545), 977–980.
Duarte, C.M., Bruhn, A., Krause-Jensen, D., 2022. A seaweed aquaculture imperative to meet global sustainability targets. Nat. Sustain. 5 (3), 185–193.
Evans, R., Lea, M.A., Hindell, M.A., Swadling, K.M., 2020. Significant shifts in coastal zooplankton populations through the 2015/16 Tasman Sea marine heatwave. Estuar. Coast. Shelf Sci. 235, 106538.
Feng, Y., Xiong, Y., Hall-Spencer, J.M., Liu, K., Beardall, J., Gao, K., Ge, J., Xu, J., Gao, G., 2024. Shift in algal blooms from micro- to macroalgae around China with increasing eutrophication and climate change. Glob. Chang. Biol. 30 (1), e17018.
Fu, F.-X., Tatters, A.O., Hutchins, D.A., 2012. Global change and the future of harmful algal blooms in the ocean. Mar. Ecol. Prog. Ser. 470, 207–233.
Gao, G., Fu, Q., Beardall, J., Wu, M., Xu, J., 2019a. Combination of ocean acidification and warming enhances the competitive advantage of *Skeletonema costatum* over a green tide alga, *Ulva linza*. Harmful Algae 85, 101698.
Gao, G., Gao, Q., Bao, M., Xu, J., Li, X., 2019b. Nitrogen availability modulates the effects of ocean acidification on biomass yield and food quality of a marine crop *Pyropia yezoensis*. Food Chem. 271, 623–629.
Gao, G., Zhao, X., Jiang, M., Gao, L., 2021. Impacts of marine heatwaves on algal structure and carbon sequestration in conjunction with ocean warming and acidification. Front. Mar. Sci. 8, 758651.
Guillard, R.R.L., Ryther, J.H., 1962. Studies of marine planktonic diatoms. I. *Cyclotella nana* Hustedt and *Detonula confervaceae* (Cleve) Gran. Can. J. Microbiol. 8, 229–239.
Heil, C.A., Muni-Morgan, A.L., 2021. Florida's harmful algal bloom (HAB) problem: escalating risks to human, environmental and economic health with climate change. Front. Ecol. Evol. 9, 646080.
Hereward, H.F.R., King, N.G., Smale, D.A., 2020. Intra-annual variability in responses of a canopy forming kelp to cumulative low tide heat stress: implications for populations at the trailing range edge. J. Phycol. 56, 146–158.
Herron, M.D., Borin, J.M., Boswell, J.C., Walker, J., Chen, I.C.K., Knox, C.A., Boyd, M., Rosenzweig, F., Ratcliff, W.C., 2019. De novo origins of multicellularity in response to predation. Sci. Rep. 9, 2328.
Hoagland, P., Kirkpatrick, B., Jin, D., Kirkpatrick, G., Fleming, L.E., Ullmann, S.G., Beet, A., Hitchcock, G., Harrison, K.K., Li, Z.C., Garrison, B., 2020. Lessening the hazards of Florida red tides: a common sense approach. Front. Mar. Sci. 7, 538.
Hobday, A.J., Alexander, L.V., Perkins, S.E., Smale, D.A., Straub, S.C., Oliver, E.C.J., Benthuysen, J.A., Burrows, M.T., Donat, M.G., Feng, M., Holbrook, N.J., Moore, P.J., Scannell, H.A., Sen Gupta, A., Wernberg, T., 2016. A hierarchical approach to defining marine heatwaves. Prog. Oceanogr. 141, 227–238.
Hoef-Emden, K., 2014. Osmotolerance in the Cryptophyceae : jacks-of-all-trades in the Chroomonas clade. Ann. Anat. 165, 123–143.
Holecek, M., 2020. Histidine in health and disease: metabolism, physiological importance, and use as a supplement Milan. Nutrients 12, 848.
Huang, Q., Li, N., Li, Y., 2021. Long-term trend of heat waves and potential effects on phytoplankton blooms in Lake Qiandaohu, a key drinking water reservoir. Environ. Sci. Pollut. Res. 28, 68448–68459.
Hwang, E.K., Yotsukura, N., Pang, S.J., Su, L., Shan, T.F., 2019. Seaweed breeding programs and progress in eastern Asian countries. Phycologia 58 (5), 484–495.
Jeong, J.H., Jin, H.J., Sohn, C.H., Suh, K.H., Hong, Y.K., 2000. Algicidal activity of the seaweed *Corallina pilulifera* against red tide microalgae. J. Appl. Phycol. 12, 37–43.
Jiang, M., Gao, L., Huang, R., Lin, X., Gao, G., 2022. Differential responses of bloom-forming *Ulva intestinalis* and economically important *Gracilariopsis lemaneiformis* to marine heatwaves under changing nitrate conditions. Sci. Total Environ. 840, 156591.
Jiang, M., Hall-Spencer, J.M., Gao, L., Ma, Z., Gao, G., 2024. Nitrogen availability regulates the effects of a simulated marine heatwave on carbon sequestration and phycosphere bacteria of a marine crop. Limnol. Oceanogr. 69 (2), 339–354.
Jones, P.M., George, A.M., 2004. The ABC transporter structure and mechanism: perspectives on recent research. Cell. Mol. Life Sci. 61, 682–699.
Kaplan, F., Guy, C.L., 2004. B-amylase induction and the protective role of maltose during temperature shock. Plant Physiol. 135, 1674–1684.
Kelly, K.J., Mansour, A., Liang, C., Kim, A.M., Mancini, L.A., Bertin, M.J., Jenkins, B.D., Hutchins, D.A., Fu, F.-X., 2023. Simulated upwelling and marine heatwave events promote similar growth rates but differential domoic acid toxicity in *Pseudo-nitzschia australis*. Harmful Algae 127, 102467.
Khotimchenko, S.V., Vaskovsky, V.E., Przhemenetskaya, V.F., 1991. Distribution of eicosapentaenoic and arachidonic acids in different species of *Gracilaria*. Phytochemistry 30, 207–209.
Kling, J.D., Lee, M.D., Fu, F.-X., Phan, M.D., Wang, X., Qu, P.P., Hutchins, D.A., 2020. Transient exposure to novel high temperatures reshapes coastal phytoplankton communities. ISME J. 14 (2), 413–424.
Li, X., 2021. Occurrence characteristics of the red tide in Fujian coastal waters during the last two decades. Mar. Environ. Sci. 40 (4), 601–610.
Li, S., Yossef, Shabtai, Arad, S.M., 2002. Floridoside as a carbon precursor for the synthesis of cell-wall polysaccharide in the red microalga *Porphyridium* sp (Rhodophyta). J. Phycol. 38, 931–938.
Li, Y., Ren, G., Wang, Q., You, Q., 2019. More extreme marine heatwaves in the China seas during the global warming hiatus. Environ. Res. Lett. 14, 104010.
Li, X., Su, L., Li, X., Li, J., Xu, Y., Chang, L., Yu, R., Yang, D., Pang, S., 2023. Comprehensive analysis of large-scale *Saccharina japonica* damage in the principal farming area of Rongcheng in Shandong Province from 2021 to 2022. J. Agr. Sci. Tech. 25, 206–222.
Liu, Q., 2015. The Interactions Study between Bloom-forming *Ulva prolifera* and Phytoplankton in the Yellow Sea. Doctoral dissertation.. Institute of Oceanology, Chinese Academy of Sciences, Qingdao.
Locher, K.P., 2016. Mechanistic diversity in ATP-binding cassette (ABC) transporters. Nat. Struct. Mol. Biol. 23, 487–493.
Lopes, V.M., Court, M., Seco, M.C., Borges, F.O., Vicente, B., Lage, S., Braga, A.C., Duarte, B., Santos, C.F., Amorim, A., Costa, P.R., Rosa, R., 2023. *Gymnodinium catenatum* paralytic shellfish toxin production and photobiological responses under marine heat waves. Toxins 15, 157.
Mohy El-Din, S.M., El-Ahwany, A.M.D., 2016. Bioactivity and phytochemical constituents of marine red seaweeds (*Jania rubens*, *Corallina mediterranea* and *Pterocladia capillacea*). J. Taibah Univ. Sci. 10, 471–484.
Nan, C., Zhang, H., Zhao, G., 2004. Allelopathic interactions between the macroalga *Ulva pertusa* and eight microalgal species. J. Sea Res. 52, 259–268.
Nepper-Davidsen, J., Andersen, D.T., Pedersen, M.F., 2019. Exposure to simulated heatwave scenarios causes long-term reductions in performance in *Saccharina latissima*. Mar. Ecol. Prog. Ser. 630, 25–39.
Oliver, E.C.J., Donat, M.G., Burrows, M.T., Moore, P.J., Smale, D.A., Alexander, L.V., Benthuysen, J.A., Feng, M., Sen Gupta, A., Hobday, A.J., Holbrook, N.J., Perkins-Kirkpatrick, S.E., Scannell, H.A., Straub, S.C., Wernberg, T., 2018. Longer and more frequent marine heatwaves over the past century. Nat. Commun. 9, 1–12.
Papanikolopoulou, L.A., Smeti, E., Roelke, D.L., Dimitrakopoulos, P.G., Kokkoris, G.D., Danielidis, D.B., Spatharis, S., 2018. Interplay between r-and K-strategists leads to phytoplankton underyielding under pulsed resource supply. Oecologia 186, 755–764.
Patil, V., Abate, R., Yang, Y., Zhang, J., Lin, H., Chen, C., Liang, J., Sun, L., Li, X., Gao, Y., 2020. Allelopathic effect of *Pyropia haitanensis* (Rhodophyta) on the bloom-forming *Skeletonema costatum* (Bacillariophyta). J. Appl. Phycol. 32, 1275–1286.
Pershing, A.J., Mills, K.E., Dayton, A.M., Franklin, B.S., Kennedy, B.T., 2018. Evidence for adaptation from the 2016 marine heatwave in the Northwest Atlantic Ocean. Oceanography 31, 152–161.
Porra, R.J., Thompson, W.A.A., Kriedemann, P.E., 1989. Determination of accurate extinction coefficients and simultaneous equations for assaying chlorophylls a and b extracted with four different solvents: verification of the concentration of chlorophyll standards by atomic absorption spectroscopy. Biochim. Biophys. Acta 975, 384–394.
Roberts, S.D., Van Ruth, P.D., Wilkinson, C., Bastianello, S.S., Bansemer, M.S., 2019. Marine heatwave, harmful algae blooms and an extensive fish kill event during 2013 in South Australia. Front. Mar. Sci. 6, 610.
Sanina, N.M., Goncharova, S.N., Kostetsky, E.Y., 2008. Seasonal changes of fatty acid composition and thermotropic behavior of polar lipids from marine macrophytes. Phytochemistry 69, 1517–1527.
Santos, M.A.Z., Colepicolo, P., Pupo, D., Fujii, M.T., de Pereira, C.M.P., Mesko, M.F., 2017. Antarctic red macroalgae: a source of polyunsaturated fatty acids. J. Appl. Phycol. 29, 759–767.
Schmid, M., Fernández, P.A., Gaitán-Espitia, J.D., Virtue, P., Leal, P.P., Revill, A.T., Nichols, P.D., Hurd, C.L., 2020. Stress due to low nitrate availability reduces the biochemical acclimation potential of the giant kelp *Macrocystis pyrifera* to high temperature. Algal Res. 47, 101895.
Shen, L., Xu, H., Guo, X., Wu, P., 2012. Oceanography of *Skeletonema costatum* harmful algal blooms in the East China Sea using MODIS and QuickSCAT satellite data. J. Appl. Remote. Sens. 6 (1), 063529.
Smale, D.A., Wernberg, T., 2013. Extreme climatic event drives range contraction of a habitat-forming species. Proc. R. Soc. B Biol. Sci. 280, 20122829.
Strickland, J.D.H., Parsons, T.R., 1972. A Practical Handbook of Seawater Analysis.
Sun, S., Hu, S., Zhang, B., Sun, X., Xu, N., 2021. Allelopathic effects and potential allelochemical of *Sargassum fusiforme* on red tide microalgae *Heterosigma akashiwo*. Mar. Pollut. Bull. 170, 112673.
Svenning, J.B., Dalheim, L., Eilertsen, H.C., Vasskog, T., 2019. Temperature dependent growth rate, lipid content and fatty acid composition of the marine cold-water diatom *Porosira glacialis*. Algal Res. 37, 11–16.
Tala, F., Chow, F., 2014. Ecophysiological characteristics of *Porphyra* spp. (Bangiophyceae, Rhodophyta): seasonal and latitudinal variations in northern-Central Chile. J. Appl. Phycol. 26, 2159–2171.
Thornton, D.C., Thake, B., 1998. Effect of temperature on the aggregation of *Skeletonema costatum* (Bacillariophyceae) and the implication for carbon flux in coastal waters. Mar. Ecol. Prog. Ser. 174, 223–231.
Uji, T., Sato, R., Mizuta, H., Saga, N., 2013. Changes in membrane fluidity and phospholipase D activity are required for heat activation of PyMBF1 in *Pyropia yezoensis* (Rhodophyta). J. Appl. Phycol. 25, 1887–1893.
Viglione, G., 2021. How heatwaves ravage the seas. Nature 593, 26–28.
Wang, Y., Yu, Z., Song, X., Tang, X., Zhang, S., 2007. Effects of macroalgae *Ulva pertusa* (Chlorophyta) and *Gracilaria lemaneiformis* (Rhodophyta) on growth of four species of bloom-forming dinoflagellates. Aquat. Bot. 86, 139–147.
Wernberg, T., 2021. Marine heatwave drives collapse of kelp forests in Western Australia. In: Canadell, J.G., Jackson, R.B. (Eds.), Ecosystem Collapse and Climate Change. Springer International Publishing, Cham, pp. 325–343.
Wernberg, T., Smale, D.A., Tuya, F., Thomsen, M.S., Langlois, T.J., De Bettignies, T., Bennett, S., Rousseaux, C.S., 2013. An extreme climatic event alters marine ecosystem structure in a global biodiversity hotspot. Nat. Clim. Chang. 3, 78–82.
Wernberg, T., Bennett, S., Babcock, R.C., De Bettignies, T., Cure, K., Depczynski, M., Dufois, F., Fromont, J., Fulton, C.J., Hovey, R.K., Harvey, E.S., Holmes, T.H., Kendrick, G., Radford, B., Santana-garcon, J., Saunders, B.J., Smale, D., Thomsen, M. S., Tuckett, C., Tuya, F., 2016. Climate-driven regime shift of a temperate marine ecosystem. Science 353, 169–172.
Yadavalli, R., Ratnapuram, H., Motamarry, S., Reddy, C.N., Ashokkumar, V., Kuppam, C., 2022. Simultaneous production of flavonoids and lipids from *Chlorella vulgaris* and *Chlorella pyrenoidosa*. Biomass Convers. Biorefinery 12, 683–691.

Yang, Y., Liu, Q., Chai, Z., Tang, Y., 2015. Inhibition of marine coastal bloom-forming phytoplankton by commercially cultivated *Gracilaria lemaneiformis* (Rhodophyta). J. Appl. Phycol. 27, 2341–2352.

Yao, Y., Wang, J., Yin, J., Zou, X., 2020. Marine heatwaves in China's marginal seas and adjacent offshore waters: past, present, and future. J. Geophys. Res.-Oceans 125 (3), e2019JC015801.

Ye, C., Liao, H., Yang, Y., 2014. Allelopathic inhibition of photosynthesis in the red tide-causing marine alga, *Scrippsiella trochoidea* (Pyrrophyta), by the dried macroalga, *Gracilaria lemaneiformis* (Rhodophyta). J. Sea Res. 90, 10–15.